Strongly Advected Jet in a Coflow

M. J. Davidson[1] and H. J. Wang[2]

Abstract: We present the results of an experimental investigation into the behavior of a strongly advected jet (weak jet) in a coflowing ambient fluid. Laser-induced-fluorescence and image processing techniques are employed to provide quantitative information about the mean properties of the flow. Data are obtained at previously inaccessible distances from the flow source, enabling the mean and fluctuating behavior of the flow in the strongly advected region to be more clearly defined. The spread relationship, traditionally employed to model the mean behavior of these flows, is redefined based on this experimental information. Both the spread constant and the ratio of the tracer to the velocity spread are shown to change in the strongly advected region. The results presented are discussed in the context of recent observations about the importance of large-scale eddy motions in defining the mean behavior of weakly advected jets and plumes. In addition the experiments provide information on the contrasts between the mixing processes in the weakly advected and strongly advected coflowing jet regions, and their influence on the mean behavior of these flows. Concentration fluctuation statistics from both regions are presented and implications for the application of the entrainment assumption in the strongly advected region are also discussed.

DOI: 10.1061/(ASCE)0733-9429(2002)128:8(742)

CE Database keywords: Jets; Flow characteristics; Data collection.

Introduction

This paper focuses on the growth of a nonbuoyant discharge in a coflowing ambient fluid, placing particular emphasis on the strongly advected region of the flow. Within this region the centreline velocity is traditionally adopted as the appropriate characteristic velocity for defining the spreading rate of the discharge (Antonia and Bilger 1974; Knudsen 1988). However, more recent studies (Wright 1994; Chu et al. 1999) have suggested that the cross-sectional spatially averaged velocity (approximately one half of the centreline velocity) is the appropriate characteristic mixing velocity and this reduces the rate of spread of the jet in the strongly advected region by a factor of 2. This issue has not been resolved because of a lack of experimental data in the strongly advected region and because of the unknown influences of ambient turbulence.

In a recent experimental investigation Nickels and Perry (1996) measured velocity fields in coflowing jets in a wind-tunnel facility. Here the impact of ambient turbulence was minimized and measurements were made in the weakly advected region and in the region where the transition from weakly to strongly advected behavior occurs. The ambient turbulence level was less than 0.6% and assumed to have no impact on the behavior of the jets in both regions. This approach is typical of traditional investigations into coflowing jets such as those conducted by Antonia and Bilger (1973); Smith and Hughes (1977); and others. A comparison of the spread data from existing experimental data sets is shown in Fig. 1. There is significant scatter in the data and this could be due in part to the impact of ambient turbulence. Indeed the impact of ambient turbulence on the mixing of jets has not yet been quantified. Data extend well into the transition region, but the expected asymptotic behavior in the strongly advected region is not yet evident. It is not therefore possible to determine with confidence the appropriate spread constant or characteristic velocity for jet mixing from existing data.

Here the results of an experimental investigation into the behavior of coflowing jets are reported. Laser-induced fluorescence (LIF) and image processing techniques are employed to accurately measure concentration profiles of a coflowing jet. Significant quantities of data are obtained in the strongly advected region, up to nondimensional distances in the region of 1,200 (previously the maximum was approximately 100). The experiments were conducted in a towing tank and carefully designed to eliminate the impact of ambient turbulence.

Discharge Configuration and Modeling Issues

As is typical for this type of problem, a coflowing jet is created when a nonbuoyant fluid discharges from a cylindrical port of diameter d_p, at an initial velocity U_0, parallel and in the same direction as the moving ambient fluid, which has a uniform velocity of magnitude U_a. The discharge may also contain a uniformly mixed tracer of concentration C_0. The release configuration is shown in Fig. 2 and it is worth noting that the coordinate x represents distances from the source in the direction of the ambient current.

Integral models for this problem have been formulated by authors such as Antonia and Bilger (1974); Knudsen (1988); and more recently Wright (1994) and Chu et al. (1999). Therefore it is not necessary to repeat the formulation here. Where these formulations differ notably, however, is in the selection of an appropriate characteristic velocity for the spread of the flow in the strongly advected region and it is this difference that provides in part the motivation for the current investigation.

[1]Dept. of Civil Engineering, Univ. of Canterbury, Private Bag 4800, Christchurch, New Zealand.

[2]Dept. of Civil Engineering, Univ. of Canterbury, Private Bag 4800, Christchurch, New Zealand.

Note. Discussion open until January 1, 2003. Separate discussions must be submitted for individual papers. To extend the closing date by one month, a written request must be filed with the ASCE Managing Editor. The manuscript for this paper was submitted for review and possible publication on March 16, 2000; approved on February 26, 2002. This paper is part of the ***Journal of Hydraulic Engineering***, Vol. 128, No. 8, August 1, 2002. ©ASCE, ISSN 0733-9429/2002/8-742–752/$8.00+$.50 per page.

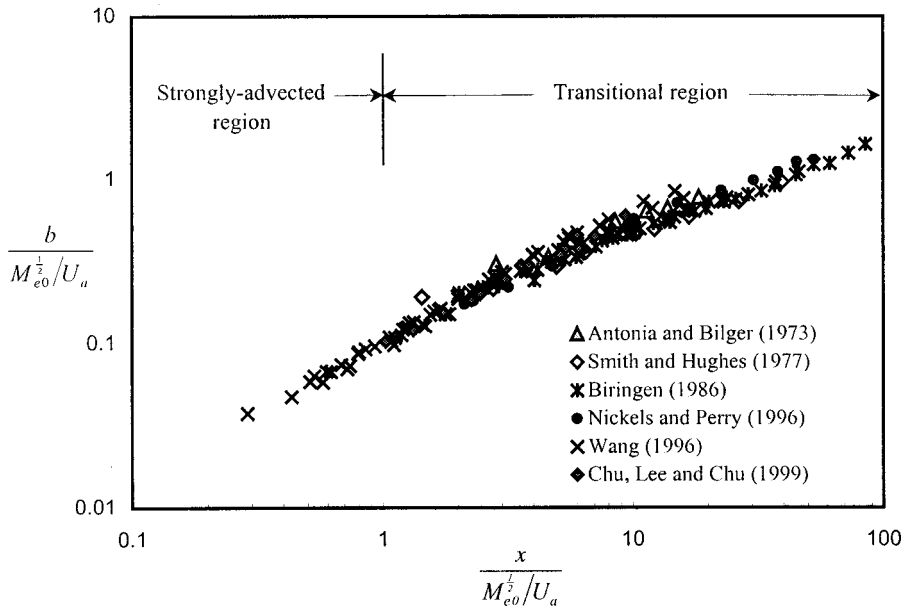

Fig. 1. Existing spread data for single jet in coflowing ambient fluid, where b is representative radius of the jet, x is distance from the flow source, U_a is ambient velocity, and M_{e0} is initial excess momentum per unit density

Recent modifications to the form of this closure equation are based on experimental investigations that have indicated the importance of large-scale structures in defining the nature of similar flows. For example, investigations by Dimotakis et al. (1983); Papantanonia and List (1989); and Davidson and Pun (1999) have shown the importance of large scale eddies in defining jet behavior. Consistent with these previous observations, during the present experimental investigation the large eddies were seen to drive the jet mixing. At a given location large eddies repeatedly form and during this formation process they entrain significant quantities of ambient fluid. This increase in eddy volume increases the scale of the jet and hence it grows. The entrained ambient fluid is mixed with the jet fluid as the large eddies break down to smaller scales.

Given the experimental evidence showing the importance of the large scale eddies in driving the entrainment process, an argument can be made for the use of the cross-sectional average velocity in the spread relationship by considering the formation of a highly idealized large eddy at a given jet cross section. Relative to the ambient motion, the large eddy is being advected by the spatially averaged excess velocity $\overline{U}_e$. Near the center of jet the fluid forming the eddy is on average (temporal) moving at the centerline excess velocity U_e. Therefore relative to the total mean motion, the central jet fluid is moving with a velocity of $U_e - \overline{U}_e \approx \overline{U}_e$. At the outer edge of the jet the mean velocity approaches 0 and hence relative to the total mean motion the velocity is $-\overline{U}_e$. The shear in the fluid therefore drives a rotation (large eddy), with velocity $\overline{U}_e$, which spans the jet radius engulfing significant quantities of ambient fluid. Hence it is the spatial mean velocity that is characteristic of the formation of large eddies, and these are the eddies responsible for the increase in the scale of the jet. It is appropriate then to relate the scale of the jet b to the characteristic velocity of large eddy motion

$$\frac{db}{dt} \sim \overline{U}_e \tag{1}$$

The mean motion of the jet fluid is given by

$$\frac{dx}{dt} = U_a + \overline{U}_e \tag{2}$$

and therefore the spread relationship can be written as

$$\frac{db}{dx} \sim \frac{\overline{U}_e}{U_a + \overline{U}_e} \tag{3}$$

Introducing a spread constant k into the equation and letting $\overline{U}_e = U_e / C_{JK}$, we can write

$$\frac{db}{dx} = k \frac{U_e}{U_e + C_{Jk} U_a} \tag{4}$$

where b = radius at which the local mean velocity equals $e^{-1} U_e$, the value of the spread constant is 0.107 (from a jet a still ambient fluid, Papanicolaou 1984) and C_{JK} has a value of approximately 2. Defining the spread relationship in this way is consistent with the work of Wright (1994) and Chu et al. (1999). In contrast, if the centerline excess velocity is adopted in the closure equation, then C_{JK} has a value of 1. The latter value was originally adopted by Patel (1971) to model the behavior of a plane jet in a coflowing ambient fluid. Antonia and Bilger (1974) and Knuden (1988) employed the same relationship when modeling the behavior of an axisymmetric jet in a coflowing ambient fluid.

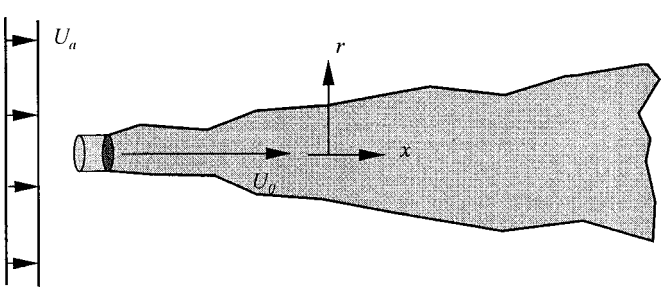

Fig. 2. Schematic diagram of jet in coflowing ambient fluid

It is perhaps useful to note at this stage that the integral formulations yield relatively simple and well-known asymptotic solutions in the weakly and strongly advected flow regions of the flow.

Weakly Advected Region: Strong Jet

In this region the initial excess momentum per unit density $[M_{e0}=\pi(U_0-U_a)U_0 d_p^2/4]$ determines the discharge behavior and the flow resembles a jet discharged into a still ambient fluid. Recognizing that the ambient velocity is very small relative to the jet centerline excess velocity gives

$$b=kx \tag{5}$$

$$\frac{U_e}{U_a}=\frac{1}{I_m^{1/2}k}\frac{M_{e0}^{1/2}/U_a}{x} \tag{6}$$

$$\frac{U_{\mathrm{ar}}}{1-U_{\mathrm{ar}}}\frac{C_0}{C}=\frac{I_{qc}k}{I_m^{1/2}}\frac{x}{M_{e0}^{1/2}/U_a} \tag{7}$$

in which C=centerline mean tracer concentration; $U_{\mathrm{ar}}=U_a/U_0$; and I_m and I_{qc}=integral constants with values of 1.74 and 1.99, respectively (see for example Davidson and Pun 1999).

Strongly Advected Region: Weak Jet

In the strongly advected region the ambient velocity plays an important role in defining the motion of the effluent. The governing parameter is the ratio of the initial excess momentum (per unit density) to the ambient velocity (M_{e0}/U_a). In this region the ambient velocity is very large relative to the jet centerline excess velocity and the integral formulation can be simplified to yield the following solution:

$$\frac{b}{M_{e0}^{1/2}/U_a}=\left(\frac{3k}{C_{Jk}I_q}\right)^{1/3}\left(\frac{x}{M_{e0}^{1/2}/U_a}\right)^{1/3} \tag{8}$$

$$\frac{U_e}{U_a}=\left(\frac{C_{Jk}^2}{I_q 9k^2}\right)^{1/3}\left(\frac{M_{e0}^{1/2}/U_a}{x}\right)^{2/3} \tag{9}$$

$$\frac{U_{\mathrm{ar}}}{1-U_{\mathrm{ar}}}\frac{C_0}{C}=I_c\left(\frac{3k}{C_{Jk}I_q}\right)^{2/3}\left(\frac{x}{M_{e0}^{1/2}/U_a}\right)^{2/3} \tag{10}$$

in which I_q $(=\pi)$ and I_c=integral constants. The value of I_c is dependent on the ratio of tracer to velocity spread λ, and this has a value of 1.19 in the weakly advected region (Fischer et al. 1979 and others) giving a value of 4.45 for the integral constant.

The solutions in the weakly and strongly advected regions provide signatures of effluent behavior, which make the weakly and strongly advected regions relatively easy to identify. The dominant parameters from the two regions combine to form a length scale X_{sw}

$$X_{\mathrm{sw}}\sim\frac{M_{e0}^{1/2}}{U_a} \tag{11}$$

This length scale provides an order of magnitude estimate of the location of the transition between weakly and strongly advected behavior. Existing experimental data indicate that the transition occurs over 2 orders of magnitude of distance, where

$$\sim 1<\frac{x}{M_{e0}^{1/2}/U_a}<\sim 100 \tag{12}$$

Thus to obtain reliable data in the strongly advected region, experimental data must be gathered at dimensionless distances well in excess of 100. Currently spread data have been gathered to a maximum dimensionless distance of 85. Thus comprehensive experimental information exists for the weakly advected and transition regions, but not the strongly advected region. Additional information can therefore be obtained by gathering experimental data within the strongly advected region of the flow.

Experimental System and Analysis Techniques

The experimental investigation was carried out in the Water Resources Research Laboratory at the Hong Kong University of Science and Technology. This laboratory houses a towing tank which is 15 m in length, 2 m wide, and 1.6 m deep. The towing tank was filled to a depth of 1.2 m with fresh water. A 1.6 or 4.7 mm diameter source pipe was attached to the computer-controlled carriage, so that it discharged horizontally at a location 600 mm below the water surface. The carriage was programmed to tow the source through the ambient fluid at a specified speed and in this way a discharge into a uniform ambient current was simulated. The source and ambient fluids were both fresh water and the densities of these fluids were accurately monitored using a precision density meter (PAAR DMA58).

A LIF system was employed to record the behavior of the jets. The light source for the system was a 6 W argon laser that was operated in a single mode at a wavelength of 514 nm. The laser light power was set at 2.0 W for these experiments. The laser beam passed through an optical fiber, which carried the beam onto the carriage of the towing tank. The optical fiber terminated where the laser beam passed onto a rotating mirror, which scanned the beam across a parabolic mirror. This combination of mirrors produced a parallel-planar light sheet. The light sheet was normally located such that its width was approximately 500 mm and its depth 5 mm in the region of interest. With this system the light sheet moved with the carriage and hence the distance from the jet source, to the portion of the jet under observation, remained constant for the duration of the experiment. Additional experiments were conducted where the light sheet remained stationary as the source moved away from the point of observation. This enabled us to observe the discharge behavior over a wide range of distances from the source. Each experiment was repeated several times, so that representative data could be obtained at locations of interest. Software tools were developed to enable concentration profiles to be extracted at fixed distances from the moving source, which requires that profiles at a particular distance from the source be tracked through a sequence of images. A more detailed description of this profile tracking system is given in Wang and Davidson (2001).

Ambient motions could have a significant impact on the behavior of the discharge in the strongly advected region. A stilling mechanism, which consisted of a 100 mm×2.0 m×1.5 m fine filter mesh, was installed in the tank to assist in dissipating motions in the receiving water. Before the beginning of each experiment, the motion of particles in the tank was observed to ensure that the receiving water was still. An additional problem is the ambient turbulence generated by the discharge structure (an approximately 2 mm or 5 mm external diameter pipe, with restraining wires). The approach taken to overcome this problem was to generate a weakly advected jet near the source. In this way ambient turbulence, generated by the discharge structure in the vicinity of the jet, was largely entrained into it in a region where its influence was negligible. This approach also ensures that the distance from the source to the strongly advected region is relatively long, al-

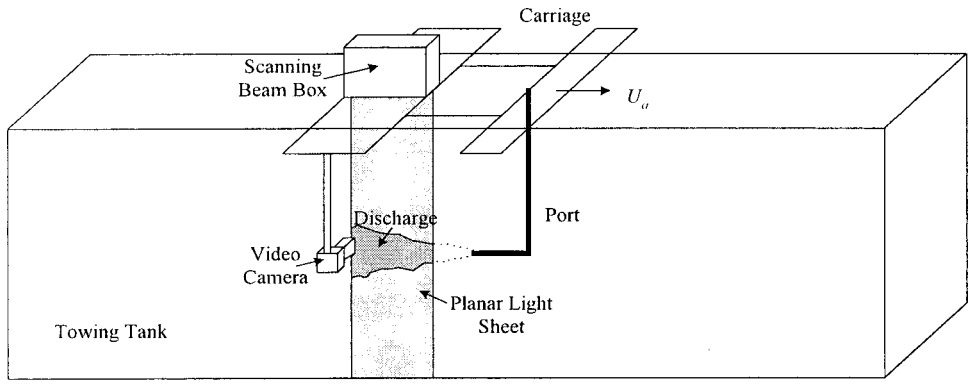

Fig. 3. Schematic diagram of laboratory facility showing towing tank and laser induced fluorescence system

lowing the ambient turbulence more time to dissipate before it can have a significant influence on jet behavior. In addition the crossflow Reynolds numbers (based on the ambient velocity and external diameter of the discharge structure) were relatively small and hence the turbulence generated was relatively weak.

Evidence to suggest that the approach taken in dealing with the pipe wake problem was successful includes the fact that the crossflow Reynolds numbers ranged from 16 to 750, but there was no appreciable difference in the behavior in the strongly advected region of the flow. In addition, if the pipe wake were to have an impact on the flow behavior it is likely to be asymmetric, with the portions of the jet directly behind the pipe being more significantly affected than those portions below the pipe. There was no evidence of asymmetry in the experimental results that would suggest the pipe wake was having a significant influence on the flow behavior.

The behavior of the jets, in the light sheet, was observed by adding a fluorescent dye tracer to the source fluid. The dye tracer was Rodamine 590; this dye fluoresces when illuminated with light of wavelength 514 nm and emits light at a wavelength of 590 nm. The observation system consisted of a low-light security video camera (Panasonic WV-BP510/G) and a video recorder (Panasonic AG-6730). The Panasonic camera was operated such that its automatic light compensation features were inactivated. The camera was fitted with a filter that eliminated light at a wavelength of 514 nm, thus the only light recorded by the observation system was that generated by the fluorescing dye. A schematic diagram of the experimental system is shown in Fig. 3. A difficulty with this type of setup is the possibility of surface waves altering the path of the light sheet. This was overcome by inserting a glass bottom open container in the free surface (not shown in Fig. 3) where the light sheet enters the receiving water.

For some of the experiments the laser sheet was turned so that a slice was taken perpendicular to the jet axis. In this situation the video camera and light sheet were also placed in a stationary position and the evolution of the jet was observed with increasing distance from the source.

The initial tracer concentration was adjusted so the jet was clearly visible to the video camera in the region of interest, while ensuring that the image was not saturated and light sheet attenuation was at acceptable levels. In the region of interest the concentrations were on the order of 0.001–0.01 mg/L, whereas as the source concentration could be has high as 1.5 mg/L. The latter value depends on the degree of dilution expected at the distance from the source where the measurements were being made. A Fluorometer (Sequoia-Turner 450) was used to monitor the initial tracer concentration in the experiments. The video images were later digitized using a Data Translation (DT2867) image capture board and processed on a PC.

The processing of the digitized images (or profiles) involved removing background light, correcting for variations in the sheet light intensity, and calibrating the image (or profile). Following this processing the intensity of light at each pixel was directly and consistently related to tracer concentration. Digitized images of a 50 mm$\times$50 mm grid were also analyzed to provide spatial calibrations for the images. Sufficient numbers of images (or profiles) were digitized such that the total sampling time was normally in excess of 50 times the large eddy advection time scale $\{b/(U_a + U_e/2)\}$. Profiles were typically extracted from video at 4 Hz because of their relatively small size, whereas complete images where sampled at 1 Hz. Averaging the digitized images (or profiles) provided details about the mean behavior of the jets. The complete set of images (or profiles) was also analyzed to provide information on fluctuation statistics, such as the root mean square and the intermittency of the concentration. Note that in the case of the concentration profiles extracted using the profile tracking system, the mean and fluctuation statistics were obtained from an ensemble of data taken from a set of identical experiments.

In some instances a correction was applied to the dilution data, which was based on tracer flux conservation (Wang 2000). Reasonable estimates of the tracer flux could be obtained in the strongly advected region without velocity measurements because the excess velocity is very small relative to the ambient velocity. In many cases the corrections required were less than 10%, but more significant corrections ($\sim$30%) were required for some data sets. The reasons for such corrections are not clear, however the fact that a single correction factor was required for a particular experiment suggests that there may have been problems with the laser light source or initial concentration measurements for those particular experiments. It is worth noting that the tracer flux corrections do not affect the spread data and that the corrected dilution data are consistent with the data that required little or no correction.

Models Predictions and Experimental Results

In presenting the experimental results we begin by considering the mean behavior of the discharge and compare our experimental results with predictions from the model outlined earlier in this paper. We then present the concentration fluctuation statistics obtained for the coflowing jets and discuss this information in the

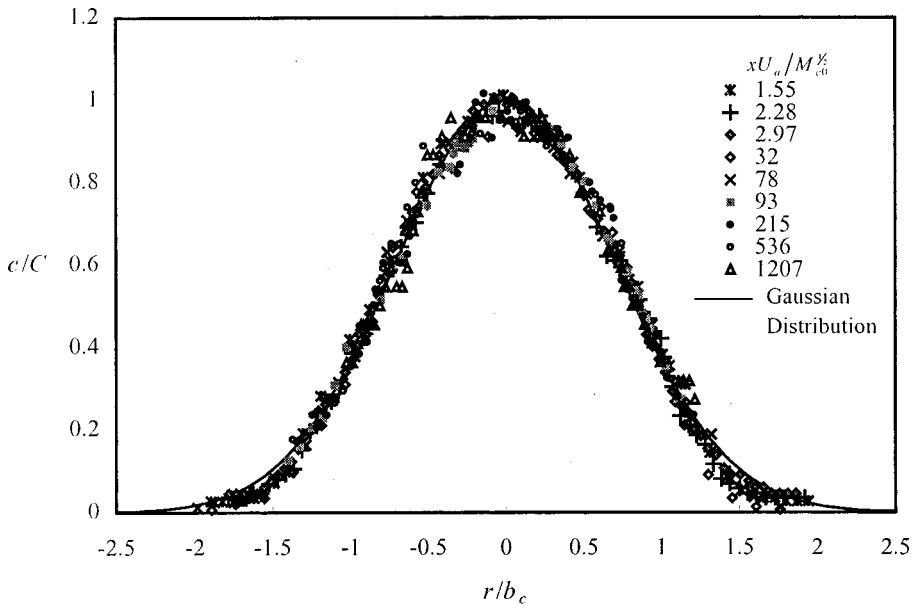

Fig. 4. Concentration profiles from coflowing jets, where $b_c = \lambda b$. Gaussian and self-similar nature of these profiles is clearly evident. Data presented are from jets with velocity ratios ranging from 0.0141 to 0.103 and port Reynolds number ranging from 2,100 to 3,300.

context of the entrainment and mixing processes in the weakly and strongly advected regions of the flow.

Mean Properties

It was assumed in developing the coflowing jet integral model that the concentration profiles are both Gaussian and self-similar. Evidence of the validity of this assumption is given in Fig. 4. Here concentration profiles are plotted from data obtained in the weakly advected region, strongly advected region, and from the transition between these two regions. The Gaussian model provides a good description of variations in the local mean concentration in all regions of the flow and the self-similar nature of the flow is also apparent from the data.

A least-squares fit of the Gaussian function to each of the concentration profiles yields the centerline concentration and representative tracer radius ($b_c = \lambda b$) of the flow, at the downstream locations where profiles have been extracted. Spread and dilution data obtained from the experiments are presented in Figs. 5 and 6. Data have been obtained at locations exceeding dimensionless distances of 1,200 from the source and hence they provide previously unseen information on the behavior of strongly advected-

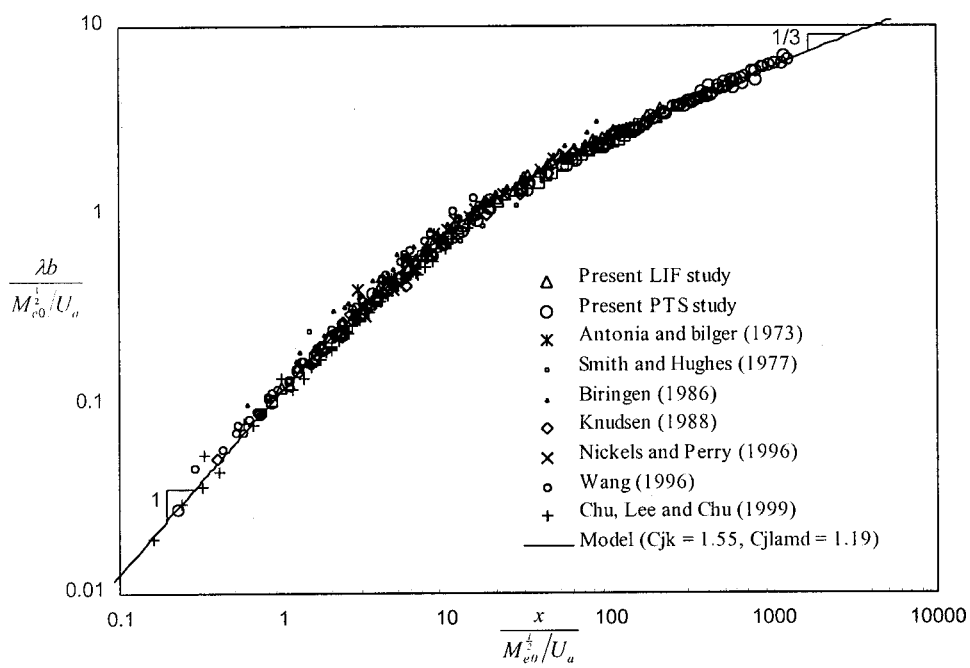

Fig. 5. Spread data obtained from laser induced fluorescence and profile tracking systems compared with model predictions. Laser induced fluorescence study: $U_{ar} = 0.0039-0.153$, $R_0 = 1{,}900-2{,}400$. Profile tracking system study: $U_{ar} = 0.0025-0.109$, $R_0 = 2{,}100-5{,}100$.

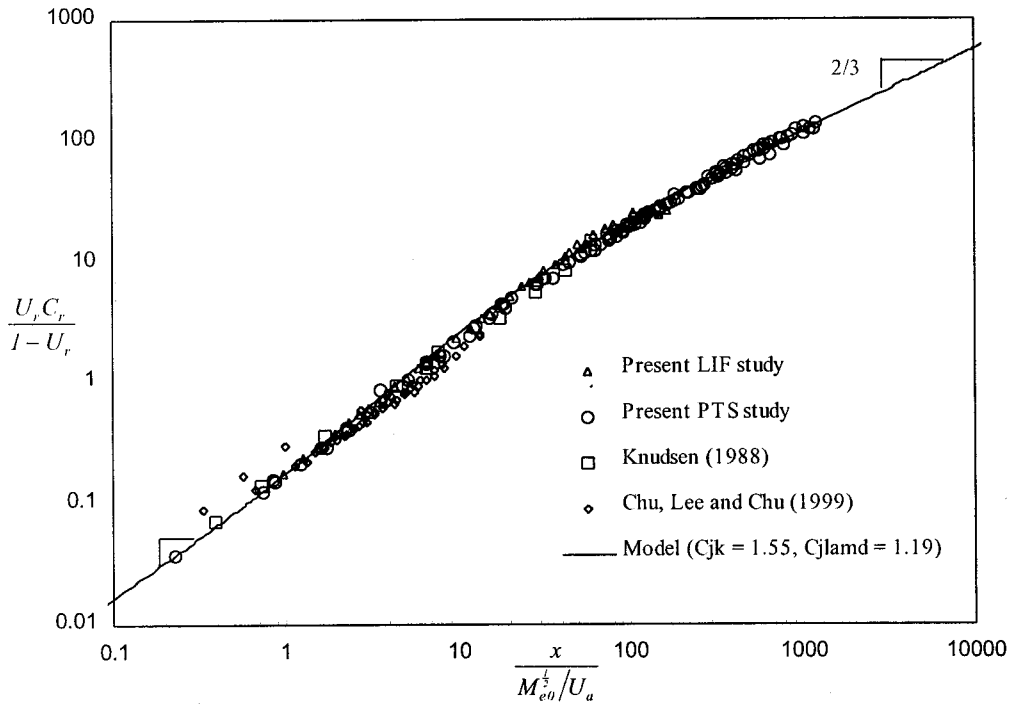

Fig. 6. Dilution data obtained from profile tracking system and laser induced fluorescence systems compared with model predictions. Laser induced fluorescence study: $U_{ar}=0.0039-0.153$, $R_0=1{,}900-2{,}400$. Profile tracking system study: $U_{ar}=0.0025-0.109$, $R_0=2{,}100-5{,}100$.

jets. However the information is in terms of tracer spread and the value of λ is not known in the strongly advected region. For this reason we alter the spread assumption [Eq. (4)] so that it is written in terms of tracer spread

$$\frac{db_c}{dx}=1.19k\frac{U_e}{U_e+C_{J\lambda}U_a} \tag{13}$$

where $C_{J\lambda}=$ constant and λ is defined by

$$\lambda=1.19\frac{U_e+C_{Jk}U_a}{U_e+C_{J\lambda}U_a} \tag{14}$$

Combining information gained from the new experimental results in Figs. 5 and 6 with information from previous velocity data (Fig. 7), the values of the constants in Eqs. (13) and (14) can

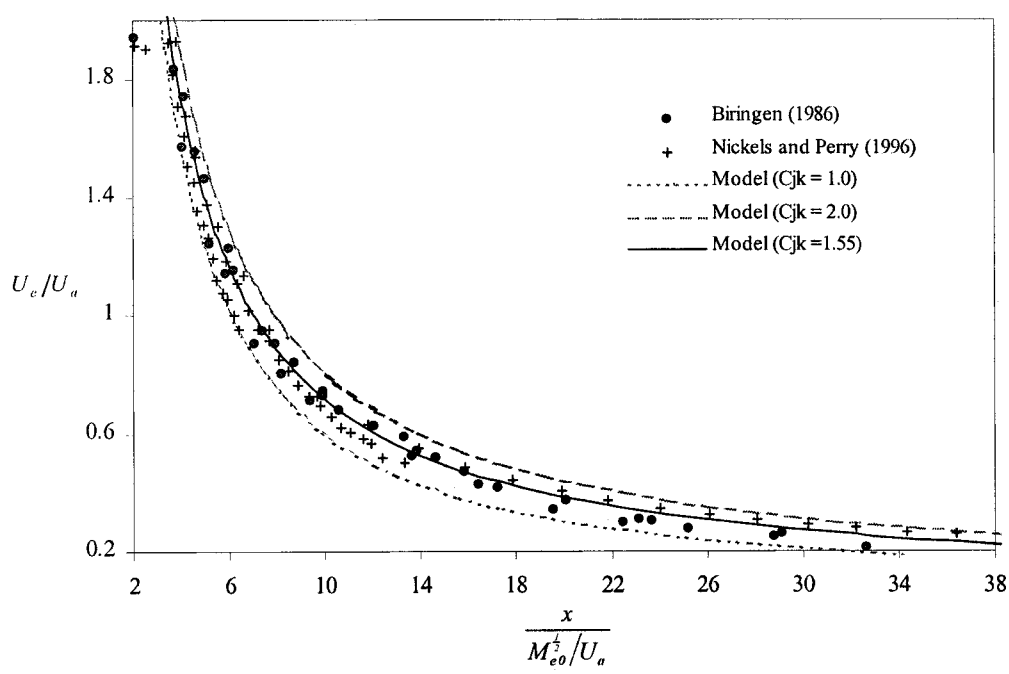

Fig. 7. Velocity data from Biringen (1986) and Nickels and Perry (1996) compared with model predictions

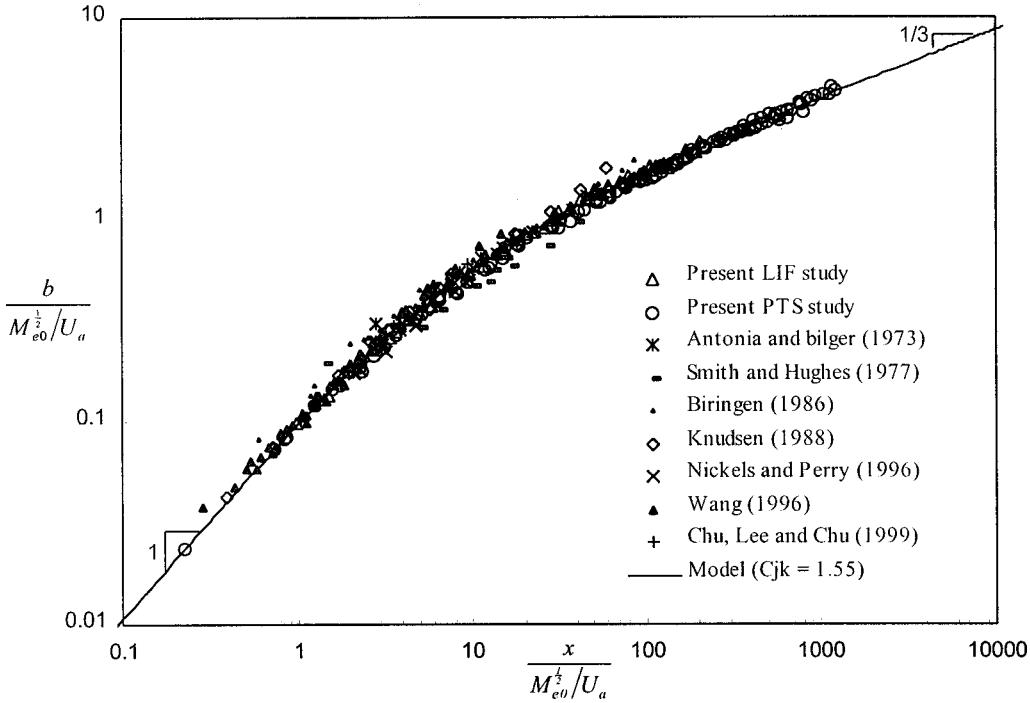

Fig. 8. Comparison of velocity spread data calculated from present study with spread data obtained in previous investigations. Laser induced fluorescence study: $U_{ar}=0.0039-0.153$, $R_0=1{,}900-2{,}400$. Profile tracking system study: $U_{ar}=0.0025-0.109$, $R_0=2{,}100-5{,}100$.

be determined as $C_{JK}=1.55$ and $C_{J\lambda}=1.19$. In Fig. 7 the model predictions are only influenced by the value of C_{JK}. Here predictions from models employing the centerline velocity ($C_{JK}=1$) and cross-sectional average velocity ($C_{JK}\approx 2$) in the closure equation are shown for comparison. It is evident that neither of these models provides particularly good predictions in the transition and strongly advected regions. The centerline velocity model has a tendency to underpredict the velocities, whereas the average velocity model overpredicts them. The data shown extends well into the transition region and has a tendency to diverge as the dimensionless distance approaches 40. However up to a dimensionless distance of approximately 20, the data sets are consistent with each other and with model predictions based on $C_{JK}=1.55$. Additional confirmation of the resulting λ values can be obtained by employing them to convert the tracer spread data, from the present study, to velocity spread data and the resulting data set is consistent with existing velocity spread data (Fig. 8). The fact that the value of C_{JK} is not the expected value (≈ 2) suggests that the spread constant k increases to a value of 0.14 in the strongly advected region.

Alternatively an entrainment assumption (Morton et al. 1956) could have been employed to close the coflowing jet problem. The use of a particular form of the spread assumption has specific implications for the form of entrainment function. The entrainment function for a jet in a coflowing ambient fluid can be written as

$$\alpha=\frac{I_q k}{\pi}\left[\left(\frac{I_m U_e}{2I_m U_e+I_q U_a}\right)\frac{U_e}{U_e+C_{Jk}U_a}+\frac{I_q}{I_m}\frac{U_a}{U_e+C_{Jk}U_a}\right] \tag{15}$$

In the weakly advected region the entrainment function collapses to the well known result $\alpha=I_q k/2\pi\approx k/2$ (List and Imberger 1973). In the strongly advected region the entrainment function collapses to $\alpha=I_q^2 k/I_m C_{JK}\pi\approx 1.16k$.

The values determined above indicate a 30% increase in the value of λ in the strongly advected region. This change is indicative of significant changes in the nature of the mixing in the strongly advected region.

Mixing Processes

Fluctuation statistics measured in a jet in a coflowing ambient fluid are shown in Figs. 9 and 10. Centerline and peak values of the root-mean-square of the concentration fluctuations are shown in Fig. 9 (profiles can be seen in Wang 2000). Near the source the centerline values resemble those obtained in a jet in still ambient fluid, that is, the maximum standard deviation is approximately 30% and in this region the profiles are self-similar. However as the nondimensional distance from the source increases the strength of the fluctuations (relative to the local mean concentration) begins to increase and self-similarity is lost. These changes suggest that the structure of the turbulence is beginning to change. Evidence of this can be seen in the transition region and well into the strongly advected region. The differences between the dimensionless root-mean-square values in the strongly and weakly advected regions are large, with the maximum approaching 100% in the strongly advected region as opposed to 30% in the weakly advected region. It is also evident that the peak values are generally higher than the centerline values in all regions of the flow. This is indicative of the double-peaked distribution that is commonly observed in the weakly advected region, but is also evident in the strongly advected region of the flow, although the data in the latter region is less consistent (Wang 2000).

Changes in the intermittency profiles with downstream distance are consistent with those observed in the dimensionless root-mean-square values and the centerline values from the intermittency profiles are shown in Fig. 10. Close to the source the intermittency values in the central regions of the jet approach 1,

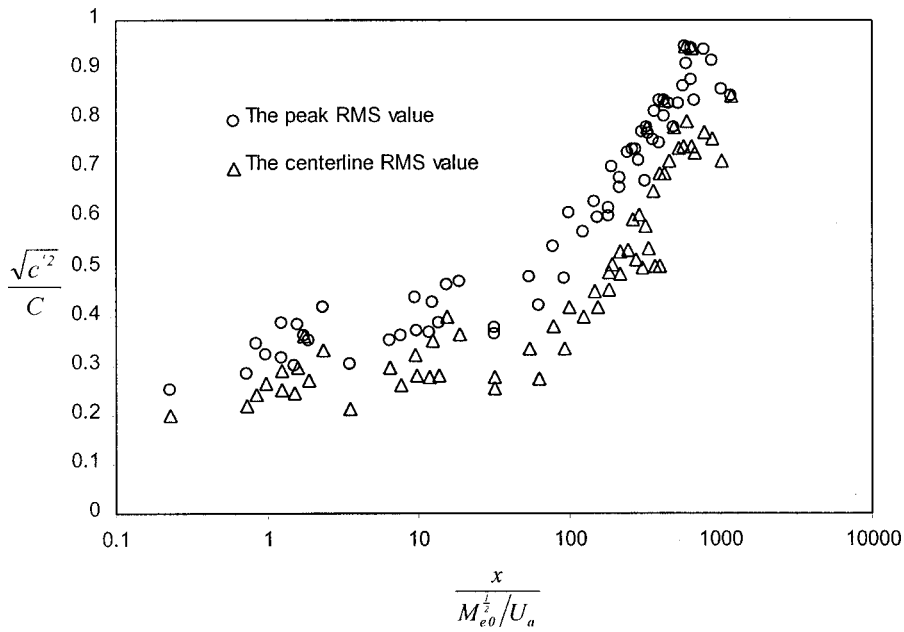

Fig. 9. Root-mean-square data obtained at a range of downstream distances in coflowing jet. Initial velocity ratio was 0.0141–0.103 and port Reynolds number was 2,100–3,300.

indicating that only a small amount of relatively pure ambient fluid reaches these regions and this is consistent with the observation of jet behavior in a still ambient fluid. However as the dimensionless distance from the source increases, and the flow enters the transition and strongly advected regions, the intermittency falls. This indicates significant changes in the turbulent structure of the flow and that the probability of finding relatively pure ambient fluid in the central regions of the flow is increasing. Again the changes are severe with the probability of *not* finding relatively pure ambient fluid in the central regions of the flow dropping from approximately 1 in the weakly advected region to 0.6 in the strongly advected region. The data also indicate that this value is continuing to fall with increasing dimensionless distance from the source. With the increased likelihood of finding ambient fluid in the central regions of the flow, the relative strength of the concentration fluctuations will increase and this is evident in the root-mean-square data in Fig. 9.

Changes in the flow structure can be seen in the images obtained during the experiments. Fig. 11 shows a sequence of images (1.0 s apart) obtained in the weakly advected region of the flow. The structure is typical of that observed in jets in a still ambient fluid. Large eddies can be seen forming, entraining significant quantities of ambient fluid, breaking up into smaller eddies, and mixing the ambient fluid with the jet fluid. These images

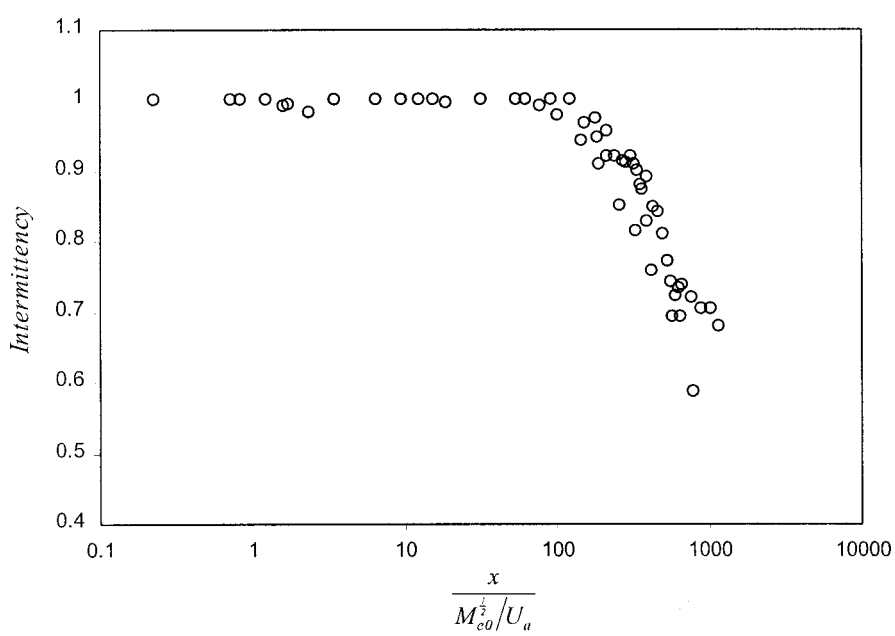

Fig. 10. Intermittency data obtained at a range of downstream distances in a coflowing jet. Initial velocity ratio was from 0.0141 to 0.103 and port Reynolds number was from 2,100–3,300. Threshold value for these calculations was set at 0.0006 mg/L.

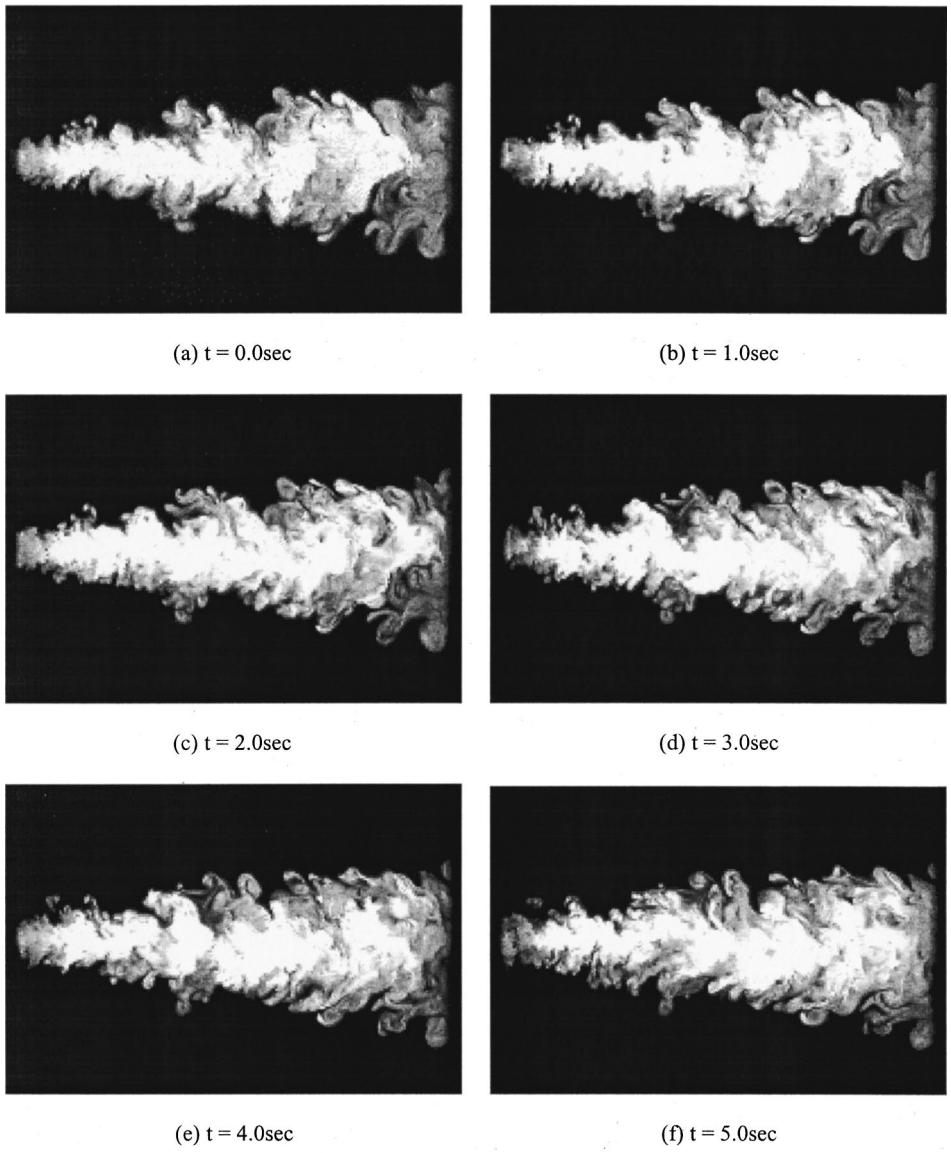

Fig. 11. Sequence of images showing complex nature of mixing processes in strongly advected region of a coflowing jet. Large eddies can be seen forming (incorporating smaller eddies from previously formed large eddies and entraining ambient fluid) and breaking down. Mixing of ambient and jet fluids by smaller scales is also apparent. Initial velocity ratio for experiment was 0.0025 and port Reynolds number was 2,150. Maximum nondimensional distance observed in images is 1.7.

also indicate the significant complexity of the mixing process. As the large eddy forms smaller eddies (resulting from the breakdown of large eddies upstream of the present location) are caught up in the formation process, as they continue to contribute to the mixing of the ambient and jet fluids. In contrast images obtained from the strongly advected region are more typical of a wake flow (Fig. 12). A sequence of essentially isolated large eddies is seen to be transported downstream by the ambient current and there is an obvious reduction in the range of eddy scales. These changes have significant impacts of the rate of dilution and energy dissipation.

The reduction in the range of eddy scales in the strongly advected region is also indicative of the flow Reynolds number becoming dependent on the downstream distance. A Reynolds number for the flow can be defined based on the centerline excess velocity and the spread of the flow. In the weakly advected region this Reynolds number is a constant with respect to distance from the source x. However in the strongly advected region this Reynolds number is proportional to $x^{-1/3}$ and therefore it reduces with increasing distance from the source, as does the range of eddy scales present in the flow. The experimental data presented in this paper was conducted for discharge Reynolds numbers (based on the initial velocity and the port diameter) ranging from 1,900 to 5,100. The value of this initial Reynolds number did not appear to have a significant influence on the flow behavior in either the weakly or strongly advected regions.

Conclusions

In this paper we have presented the results of an experimental investigation into the behavior of a nonbuoyant discharge in a coflowing ambient fluid. Laser-induced fluorescence and image processing techniques have been employed to obtain concentration data and we have placed an emphasis on obtaining experimental data in the strongly advected region of the flow, where

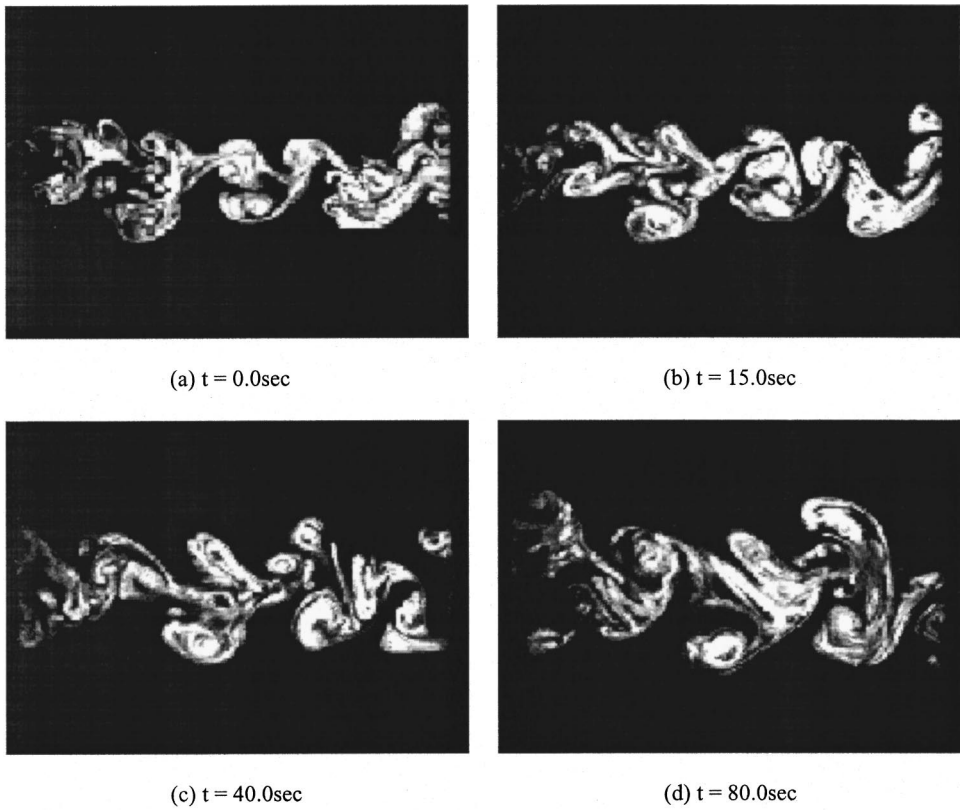

Fig. 12. Sequence of images showing flow structure in strongly advected region. Initial velocity ratio for experiment was 0.103 and port Reynolds number was 2,100. Maximum nondimensional distance observed in images is 700.

limited information exists about the flow behavior. Data have been obtained at dimensionless distances that are at least an order of magnitude greater than previous investigations.

Mean concentration profiles have provided information on the spread and dilution of the discharge. In the strongly advected region we have provided evidence that the spread relationship should be modified to allow for the fact that the spread constant changes in this region. An entrainment function that provides the same solution as the modified form of the spread function has also been presented. In addition the results suggest that changes in the structure of the flow in the strongly advected region result in an increase in the difference between the spread of the velocity and concentration profiles.

Fluctuation statistics have been obtained in the weakly advected, transition, and strongly advected coflowing jets. The dimensionless root mean square of the concentration fluctuations in the central regions of the flow is seen to increase significantly as the flow enters the transition and then strongly advected regions. Consistent with this is a significant reduction in the intermittency within the jet in these regions. Increased quantities of relatively pure ambient fluid are able to enter the central regions of the flow because of the changing jet structure and hence the probability of not finding ambient in these regions is reduced, whereas the strength of the fluctuations increases (relative to the local mean concentration). These observations are supported by images showing the turbulent structure of the flows recorded in the weakly and strongly advected regions. There is an obvious reduction in the range of eddy scales in the strongly advected region, which is consistent with the reducing flow Reynolds number in this region.

Acknowledgment

The writers acknowledge the financial support of the Research Grants Council of Hong Kong.

Notation

The following symbols are used in this paper:

b = velocity spread of jet;
b_c = concentration spread of jet;
C = centerline tracer concentration;
C_{JK} = velocity spread constant;
$C_{J\lambda}$ = concentration spread constant;
C_0 = initial tracer concentration;
d_p = diameter of discharge port;
I_m, I_q, I_c, and I_{qc} = shape constants;
k = spread constant;
M_{e0} = initial excess momentum of jet;
Q_0 = initial volume flow rate;
R_0 = discharge Reynolds number;
U_a = ambient fluid velocity;
U_{ar} = ambient to initial discharge velocity ratio;
U_e = centerline temporal mean excess velocity of jet;
$\overline{U_e}$ = cross-sectional spatially averaged excess velocity of jet;
U_0 = magnitude of initial absolute flow velocity vector;

X_{SW} = length scale for the transition between weakly advected jet and strongly advected jet regions;
x = Cartesian coordinate in same direction as ambient velocity and distance from jet virtual source;
α = entrainment coefficient; and
λ = difference in width of velocity and tracer concentration distributions.

References

Antonia, R. A., and Bilger, R. W. (1973). ''An experimental investigation of an axisymmetric jet in a coflowing air stream.'' *J. Fluid Mech.*, 61, 805–822.

Antonia, R. A., and Bilger, R. W. (1974). ''The prediction of the axisymmetric turbulent jet issuing into a coflowing stream.'' *Aeronaut. Q.*, 251, 69–80.

Biringen, S. (1986). ''An experimental investigation of a turbulent round jet in a coflowing airstream.'' *Proc., ASME Winter Annual Meeting*, Anaheim, Calif.

Chu, V. H. (1994). ''Lagrangian scaling of turbulent jets and plumes with dominant eddies.'' *Recent research advances in the fluid mechanics of turbulent jets and plumes*, Kluwer Academic, Dordrecht, The Netherlands, 45–72.

Chu, P. C. K., Lee, J. H., and Chu, V. H. (1999). ''Spreading of turbulent round jet in coflow.'' *J. Hydraul. Eng.*, 125(2), 193–204.

Davidson, M. J., and Pun, K. L. (1999). ''Weakly advected jets in crossflow.'' *J. Hydraul. Eng.*, 125(1), 47–58.

Dimotakis, P. E., Miake-Lye, R. C., and Papantoniou, D. A. (1983). ''Structure and dynamics of round turbulent jets.'' *Phys. Fluids*, 26(11), 3185–3192.

Fischer, H. B., List, E. J., Koh, R. C. Y., Imberger, J., and Brooks, N. H. (1979). *Mixing in inland and coastal waters*, Academic, New York.

Knudsen, M. (1988). ''Buoyant horizontal jets in an ambient flow.'' PhD thesis, Univ. of Canterbury, Christchurch, New Zealand.

List, E. J., and Imberger, J. (1973). ''Turbulent entrainment in buoyant jets and plumes.'' *J. Hydraul. Div., Am. Soc. Civ. Eng.*, 99(9), 1461–1474.

Morton, B., Taylor, G. I., and Turner, J. S. (1956). ''Turbulent gravitational convection from maintained and instantaneous sources.'' *Proc. R. Soc. London, Ser. A*, 234, 1–23.

Nickels, T. B., and Perry, A. E. (1996). ''An experimental and theoretical study of the turbulent coflowing jet.'' *J. Fluid Mech.*, 309, 157–182.

Papanicolaou, P. N. (1984). ''Mass and momentum transport in a turbulent buoyant vertical axisymmetric jet.'' PhD thesis, California Institute of Technology, Pasadena, Calif.

Papantoniou, D., and List, E. J. (1989). ''Large-scale structure in the far field of buoyant jets.'' *J. Fluid Mech.*, 209, 151–190.

Patel, R. P. (1971). ''Turbulent jets and wall jets in uniform streaming flow.'' *Aeronaut. Q.*, 22, 311–326.

Smith, D. J., and Hughes, T. (1977). ''Some measurements in a turbulent circular jet in the presence of a coflowing free stream.'' *Aeronaut. Q.*, 28, 185–196.

Wang, H. J. (2000). ''Jet interaction in a still or coflowing environment.'' PhD thesis, Hong Kong Univ. of Science and Technology, Hong Kong.

Wang, H. J., and Davidson, M. J. (2001). ''A profile tracking system for investigations into the behaviour of discharges in moving environments.'' *Exp. Fluids*, 31, 533–541.

Wright, S. J. (1994). ''The effect of ambient turbulence on jet mixing.'' *Recent research advances in the fluid mechanics of turbulent jets and plumes*, P. A. Davies and M. J. Valente Neves, eds., Kluwer Academic, Dordrecht, The Netherlands, 13–27.